EBioMedicine 43 (2019) 513–524

Contents lists available at ScienceDirect

EBioMedicine

journal homepage: www.ebiomedicine.com

EBioMedicine
Published by THE LANCET

CD5L is a pleiotropic player in liver fibrosis controlling damage, fibrosis and immune cell content

Cristina Bárcena [a,1], Gemma Aran [a,1], Luís Perea [b], Lucía Sanjurjo [a,c], Érica Téllez [a], Anna Oncins [a], Helena Masnou [d], Isabel Serra [d], Mónica García-Gallo [e], Leonor Kremer [e], Margarita Sala [d,f], Carolina Armengol [f,g], Pau Sancho-Bru [b,f], Maria-Rosa Sarrias [a,f,*]

[a] Innate Immunity Group, Health Sciences Research Institute Germans Trias i Pujol (IGTP), Badalona, Spain
[b] Institut d'Investigacions Biomèdiques August Pi i Sunyer (IDIBAPS), Barcelona, Spain
[c] Network for Biomedical Research in Diabetes and Associated Metabolic Disorders (CIBERDEM), Spain
[d] Gastroenterology Dept., University Hospital Germans Trias i Pujol (HUGTiP), Badalona, Spain
[e] Protein Tools Unit and Department of Immunology and Oncology, Centro Nacional de Biotecnologia (CNB-CSIC), Madrid, Spain
[f] Network for Biomedical Research in Hepatic and Digestive Diseases (CIBERehd), Spain
[g] Childhood Liver Oncology Group, Program of Predictive and Personalized Medicine of Cancer (PMPCC), IGTP, Spain

ARTICLE INFO

Article history:
Received 18 February 2019
Received in revised form 17 April 2019
Accepted 26 April 2019
Available online 8 May 2019

Keywords:
Macrophage
Apoptosis inhibitor of macrophages
TGFB
Hepatic stellate cells
SMAD7

ABSTRACT

Background: Chronic hepatic inflammation leads to liver fibrosis, which may progress to cirrhosis, a condition with high morbidity. Our aim was to assess the as yet unknown role of innate immunity protein CD5L in liver fibrosis.

Methods: CD5L was measured by ELISA in plasma samples from cirrhotic ($n = 63$) and hepatitis ($n = 39$) patients, and healthy controls ($n = 7$), by immunohistochemistry in cirrhotic tissue ($n = 12$), and by quantitative RT-PCR in mouse liver cell subsets isolated by cell sorting. Recombinant CD5L (rCD5L) was administered into a murine model of CCl_4-induced fibrosis, and damage, fibrosis and hepatic immune cell infiltration, including the $LyC6^{hi}$ (pro-fibrotic)-$LyC6^{low}$ (pro-resolutive) monocyte ratio were determined. Moreover, rCD5L was added into primary human hepatic stellate cells to study transforming growth factor β (TGFβ) activation responses.

Findings: Cirrhotic patients showed elevated plasma CD5L concentrations as compared to patients with hepatitis and healthy controls (Mann-Whitney test $p < 0{\cdot}0001$). Moreover, plasma CD5L correlated with disease progression, FIB4 fibrosis score (r:0·25, $p < 0{\cdot}0001$) and tissue expression ($r = 0{\cdot}649$; $p = 0{\cdot}022$). Accordingly, CCl_4-induced damage increased CD5L levels in total liver, particularly in hepatocytes and macrophages. rCD5L administration attenuated CCl_4-induced injury and fibrosis as determined by reduced serum transaminase and collagen content. Moreover, rCD5L inhibited immune cell infiltration and promoted a phenotypic shift in monocytes from $LyC6^{hi}$ to $LyC6^{low}$. Interestingly, rCD5L also had a direct effect on primary human hepatic stellate cells promoting SMAD7 expression, thus repressing TGFβ signalling.

Interpretation: Our study identifies CD5L as a key pleiotropic inhibitor of chronic liver injury.

Fund: Fundació Marató TV3, AGAUR and the ISCIII-EDRF.

Abbreviations: ALT, aspartate transaminase; APRI, AST to platelet ratio index; AST, aspartate aminotransferase; bHLH, basic helix-loop-helix; BMP, bone morphogenetic proteins; CCl_4, carbon tetrachloride; CD5L, CD5-like protein; ECM, extracellular matrix; ELISA, enzyme-linked immunosorbent assay; EMT, epithelial mesenchymal transition; FBS, fetal bovine serum; FIB4, fibrosis-4 score; H&E, haematoxylin and eosin; HCC, hepatocellular carcinoma; HCV, hepatitis C virus; hHSC, human primary HSC; HMDMs, human monocyte-derived macrophages; hSA, human albumin; HSC, hepatic stellate cells; Id, inhibitor of DNA binding/differentiation; ID2, DNA-binding protein inhibitor ID-2; ID3, DNA-binding protein inhibitor ID-3; IHC, immunohistochemistry; IHIC, intrahepatic immune cells; LDH, lactate dehydrogenase high; LX2, human immortalized HSCs; mAb, monoclonal; MAPK, mitogen-activated protein kinase; MDM, monocyte-derived macrophage; MPO, myeloperoxidase; NAFLD, non-alcoholic fatty liver disease; NLRP3, NOD-like receptor protein 3; SMAD, mothers against decapentaplegic homolog; TGFβ, transforming growth factor β; VEGF, vascular endothelial growth factor; αSMA, alpha smooth muscle actin.

* Corresponding author at: Innate Immunity Group, Health Sciences Research Institute Germans Trias i Pujol. Ctra Can Ruti, Camí de les Escoles s/n, Edifici Muntanya, Planta 2, 08916 Badalona, Spain.
E-mail address: mrsarrias@igtp.cat (M.-R. Sarrias).

[1] Equal contribution.

https://doi.org/10.1016/j.ebiom.2019.04.052

Research in context

Evidence before this study

Persistent inflammation of the liver leads to hepatic fibrosis, which at later stages can cause severe morbidity. CD5-like protein (CD5L) is a soluble protein that circulates in blood. Previous studies suggested that high serum/plasma levels of this protein correlate with liver damage in chronic liver disease.

Added value of this study

In this study we have reinforced the notion that CD5L plasma levels increase with disease severity. Our data further suggest that CD5L could be a biomarker of liver fibrosis. Moreover, using an experimental mouse model of liver fibrosis and hepatic stellate cell isolated from human livers, we have elucidated the role of CD5L in these settings. We have found that CD5L attenuates liver damage and fibrosis and lowers immune cell infiltration to the liver. Thus, CD5L is a key player controlling liver fibrosis.

Implications of all the available evidences

Our results complete the previous studies and confirm that CD5L detection in plasma could be used as a biomarker for liver fibrosis stages, which would be a helpful resource for the clinical management of liver disease. Besides, we provide evidence that the administration of CD5L during liver damage generates a response that seeks to counteract the inflammatory and profibrotic responses. Our data could be the basis for new CD5L-based therapies targeting liver fibrosis.

1. Introduction

Hepatic fibrosis is a dynamic process in which chronic injury of any etiology, including viral infection, alcoholic consumption and steatosis, causes persistent inflammation and leads to the accumulation of extracellular matrix (ECM) and at later stages can cause severe morbidity and mortality. The progression of fibrosis is a complex orchestrated process that involves the recruitment of many cell types, as well as cross talk between them. However, the key cellular event initiating liver fibrogenesis is the activation of local resident hepatic stellate cells (HSCs), which transdifferentiate from quiescent, vitamin-A-storing cells into proliferative, fibrogenic myofibroblasts [1]. The correct regulation of HSCs activation is key in preventing that tissue repair progresses to cirrhotic disease. The latter is characterised by a distortion of the liver parenchyma and vascular architecture, and can lead to the development of portal hypertension and clinical complications, such as oesophagic varices, ascites, and hepatocellular carcinoma (HCC) [2].

In the hepatic microenvironment, transforming growth factor β1 (TGFβ1) is one of the most potent pro-fibrogenic cytokines, and it plays a central role in hepatic fibrosis [3]. Signalling of the TGFβ family (which includes TGFβ and bone morphogenetic proteins (BMP)) occurs through phosphorylation of TGFβ (I/II) or BMP receptors, thereby activating intracellular downstream mothers against decapentaplegic homolog (SMADs). Specifically for TGFβ1 activation of HSCs, the canonical pathway is activated upon binding to the TGFβRII receptor, hetero-dimerization and activation of the TGFβRI-kinase, and subsequent phosphorylation of SMAD2/3. The latter then translocate into the nucleus, where they co-regulate the transcription of a large group of genes [4], including fibrogenic components (collagens), epithelial mesenchymal transition (EMT) markers (αSMA and E-cadherin), and angiogenic factors (VEGF) [5,6]. This signalling is modulated by inhibitory SMADs (I-Smads), such as SMAD7, which play a negative role in a feedback-regulatory manner [5,6], and by numerous factors and pathways, including the mitogen-activated protein kinase (MAPK) [7,8]. Moreover, BMP ligands such as BMP7 and 9 may also modulate HSC activity by interfering with or potentiating TFGβ signalling, respectively [9].

CD5-like protein (CD5L) is a 40-kDa soluble glycoprotein that is produced mainly by macrophages. CD5L plays diverse roles at the intersection between lipid homeostasis and the immune response, being involved in processes such as infection, atherosclerosis and cancer [10,11]. CD5L expression in macrophages is upregulated under inflammatory conditions of infectious origin such as *Listeria monocytogenes* [12,13] and *Mycobacterium tuberculosis* infection [14,15], and also in atherosclerotic lesions [16]. Interestingly, CD5L is also produced by other immune cells, such as Th17 cells [17], as well as epithelial cells of the lung [18] and retina [19].

Regarding CD5L function in the liver, early studies using a mouse model of LPS-induced hepatitis suggested that CD5L supports macrophage survival and phagocytic activity, thus enhancing efficient clearance of dead cells and infectious or toxic reagents [20]. Additionally, in the setting of HCC, we have recently shown that CD5L is expressed both by macrophages and hepatocytes in tumour and adjacent cirrhotic tissue. Moreover, elevated expression of CD5L in tumour tissue correlates with poor patient prognosis and higher tumour proliferation. *In vitro*, we showed that CD5L enhances the proliferation of liver cancer cells and protects them from apoptosis [21]. However, whether CD5L participates in earlier stages of liver pathogenesis during chronic injury, specifically liver fibrosis has not been addressed to date.

In addition to being expressed in tissue under inflammatory conditions, CD5L is detected in high amounts in serum/plasma, where it circulates in association with IgM [10]. Interestingly, in chronic liver disease, high serum/plasma levels of this protein correlate with liver damage in patients with Hepatitis C Virus (HCV), Non Alcoholic Fatty Liver Disease (NAFLD) [22–25] and HCC [26]. Whether the liver is the source of circulating CD5L in these clinical conditions remains to be elucidated.

In the present study, we observed that CD5L plasma levels were significantly elevated in a cohort of HCV and alcoholic cirrhotic patients and that they correlated with moderate and advanced fibrosis. *In vivo*, administration of rCD5L attenuated liver injury, namely ECM deposition, as well as inflammatory cell recruitment and macrophage phenotype. Moreover, by acting in a paracrine way, CD5L was able to downregulate the fibrogenic capacity of HSCs by inhibiting the TGFβ pathway. Together, our results suggest that CD5L is a key player in liver fibrogenesis.

2. Materials/patients and methods

2.1. Patients

All human studies were conducted following the Declaration of Helsinki principles and current legislation on the confidentiality of personal data and were approved by the Human Ethics Committee of the Hospital Universitari Germans Trias i Pujol (HuGTiP) and by the Ethics Committee of the Hospital Clinic of Barcelona (for primary HSC isolation, see below). Retrospective plasma samples from healthy controls ($n = 7$) and patients with chronic hepatitis ($n = 39$) and cirrhosis ($n = 63$) and formalin-fixed paraffin-embedded tissue were obtained from HuGTiP. The healthy controls had no history of liver disease, no viral hepatitis, and no malignant disease. In addition, abdomen ultrasound was performed in all healthy participants in this study at inclusion to rule out any liver disease. Buffy coats, provided by the Blood and Tissue Bank (Barcelona, Spain), were obtained from healthy blood donors following the institutional standard operating procedures for blood donation and processing, including informed consent.

2.2. Immunohistochemistry analysis

Immunohistochemical analysis of CD5L staining of cirrhotic tissue has been described before [21]. Additional information is provided in Supplementary Methods.

2.3. Animal procedures

Animal care and treatment were carried out in accordance with Spanish and EU laws. The CSIC Ethics Committee approved these experiments and the Community of Madrid Agriculture Department approved the use of experimental animals PROEX 18/14 to LK for monoclonal (mAb) generation, and the Animal Experimentation Ethics Committee at the University of Barcelona (for animal models of liver fibrosis).

2.4. MAb generation and ELISA assays

Murine mAbs against human CD5L were raised by subcutaneous immunization of BALB/c mice with 25 μg of a KLH-coupled rCD5L, produced in our laboratory [27], using standard procedures [28,29]. Further detail is provided in Supplementary Methods. Positive hybridomas were cloned by limiting dilution. mAbs were produced in tissue culture supernatants and purified by affinity chromatography using Protein G-Sepharose (GE Healthcare). The immunoglobulin subclass was determined by ELISA using specific peroxidase-conjugated antibodies against the heavy chain of mouse immunoglobulins (IgG1, IgG2a, IgG2b, IgG3 and IgM). The two mAbs were IgG1. ELISA assays to screen anti-CD5L antibodies and to measure plasma CD5L concentrations are described in Supplementary Methods. The lower limit detection of the ELISA was 0·625 ng/ml. The measurement range was 0·625 to 80 ng/ml, with an intra- and interassay precision of 2·4% and 5·8%, respectively.

2.5. In vivo induction of liver injury

Experiments were performed with 8- to 12-week-old male mice C57BL/6 (Charles River, l'Arbresle, France) (RRID:IMSR_CRL:27). To induce chronic liver injury, mice were treated with carbon tetrachloride (CCl_4) injected intraperitoneally at a dose of 0·5 ml/Kg twice a week for two weeks; control mice were injected with corn oil. Sample size was determined according to previous experiments using the same model [30]. To assess the effect of CD5L on chronic liver injury, we used endotoxin-free rCD5L [27], (see Supplementary Methods). rCD5L (25 μg) or vehicle (Saline) was administered three times by intraperitoneal (IP) injection, starting after the second injection of CCl_4/control (at days 6, 9 and 12 of the experiment). Mice were sacrificed 48 h after the last injection of CCl_4. Liver damage was determined with haematoxylin and eosin (H&E) staining of resected livers, as well as *via* serological markers (ALT, AST and LDH), analysed by the Centro de Diagnóstico Médico (Hospital Clinic, Barcelona, Spain).

2.6. Isolation of mouse hepatic cell populations

Mouse hepatic cell populations were isolated and FACS-sorted. Cells were isolated by a two-step collagenase-pronase perfusion of livers followed by Nycodenz density gradient centrifugation, as previously described [30]. The cells obtained were incubated with CD3-FITC (eBioscience, Affymetrix, San Diego, CA, USA) (RRID:AB_2572430) (T cells), F4/80-Alexa Fluor 647 (Bio-Rad, Oxford, UK) (RRID:AB_323931) (macrophages) and Ly6G-APC (eBioscience) (RRID:AB_2573307) (neutrophils). HSCs were identified on the basis of vitamin A content, and the different populations were isolated by flow cytometry, as previously described [30], using a high-speed FACS-Aria cell sorter (BD, New Jersey, NJ, USA).

2.7. Liver histopathology

Mice were anesthetized with ketamine, and blood and liver were immediately harvested. Livers were washed in PBS, and tissue samples for histology, RNA and protein extract were collected. Livers were fixed with 4% paraformaldehyde in PBS and embedded in paraffin. Liver sections were stained with primary anti-αSMA (1:500, Abcam) (RRID:AB_870573) or Myeloperoxidase, MPO (1:50, Abcam) (RRID: AB_307322) antibodies overnight at 4 °C. Liver damage or ECM deposition was determined by H&E or Masson's trichrome staining, respectively, following standard procedures. Immunohistochemistry microscopy images were taken with a Nikon Eclipse E600 microscope. Staining levels were quantified in 10 fields for each section and quantified using the Image J software as before [30]. Results were expressed as percentage (%) of positive area.

2.8. Mechanical disruption of the liver and subsequent isolation of intrahepatic immune cells (IHICs)

IHICs were isolated by mechanical disruption. In this regard, the liver was minced into small pieces with surgical scissors and then forced gently through 70-μm cell strainers using a sterile syringe plunger and RPMI containing 2% FCS. The suspensions were then centrifuged at 60 *g* for 1 min at rt. Supernatants were then pelleted by centrifugation at 400 *g* and subjected to two cycles of washing with RPMI containing 2% FCS. Pellets were resuspended in RPMI containing 2% FCS, and

Table 1
Baseline characteristics of healthy donors, chronic hepatitis and cirrhotic patients included in the study.

	Healthy (n:7)	Chronic hepatitis (n:39)	Cirrhotic (n:63)
Gender	M: 4 / F: 4	M: 21 / F: 18	M: 34 / F: 29
Age (years)	54·2 ± 17·2 [20–71]	56 ± 11 [33–74]	63·3 ± 10·4 [42–78]
Etiology	–	HCV:39/ HBV:0 / NASH:0 / OH:0	HCV:47 / HBV:3 / NASH:4 / OH:9
Varicose veins	–	–	No: 18 / Yes: 45
Ascites	–	–	No: 42 / Yes: 21
Child pugh	–	–	A: 45 / B: 17 / C: 1
ALT (U/l)	23 ± 9·5 [16–37]	62 ± 36 [23–142]	58·4 ± 40·5 [13–165]
AST (U/l)	21·7 ± 6·8 [18–32]	47·3 ± 23·5 [47–23]	65 ± 35·4 [1·9–183]
GGT (U/l)	18·2 ± 2·8 [14–20]	80 ± 56·7 [14–454]	106·9 ± 137·9 [13–785]
Alkaline phosphatase (U/l)	65·5 ± 5·5 [60–72]	72·7 ± 20·9 [42–133]	103·3 ± 44·6 [44–180]
Total bilirrubin (mg/dl)	0·4 ± 0·2 [0·2–0·7]	0·58 ± 0·26 [0·25–1·24]	1·3 ± 0·8 [0·4–3·9]
Albumin (g/l)	43·2 ± 1·9 [41·1–44·7]	41·6 ± 2·8 [35–46·6]	36·8 ± 4·7 [26·2–47·9]
Prothrombin time (%)	100 ± 0 [100−100]	97 ± 5·5 [78–100]	84·5 ± 12 [60–100]
Na (mEq/l)	142 ± 2·3 [140–144]	141 ± 2·6 [136–150]	139·8 ± 3·9 [123–147]
Platelets (10^9/l)	187·9 ± 30 [141–217]	199 ± 45 [156–292]	98·6 ± 62·2 [28–501]

For parametric variables, mean ± SD as well as the range of diversity are presented.
Abbreviations: M, male; F, female; HCV, hepatitis C virus; HBV, hepatitis B virus; NASH, Non-alcoholic steatohepatitis; OH, alcohol; −, Not Applicable; ALT, alanine aminotransferase; AST, aspartate aminotransferase; GGT, gamma-glutamyltransferase; Na, sodium.

peripheral blood mononuclear cells were then isolated by density gradient centrifugation through Ficoll-Paque (GE Healthcare) at 400 *g* for 30 min. Cellular suspensions were washed in RPMI containing 2% FCS, resuspended in 2 ml ammonium chloride/Tris-chloride (pH 7·2) (erythrocyte lysing buffer), and incubated at rt. for 5 min. They were then supplemented with 1 ml FCS and centrifuged at 400 *g*. Finally, cell pellets were resuspended in 1 ml ice cold PBS containing 2% FCS and 0.1% NaN_3 (FACS buffer) and subjected to cell surface phenotyping by flow cytometry.

2.9. Immunofluorescent staining and flow cytometry analysis

IHICs were incubated with antibodies (all from BD Biosciences, San Jose, CA, USA) for 30 min at 4 °C. Group A antibodies comprised anti-CD11b-Alexa647 (RRID:AB_396796), anti-LY6G-FITC (RRID:AB_1036098), anti-F4/80-PE (RRID:AB_2687527), and anti-LY6C- BV421 (RID:AB_2737748). Group B antibodies comprised anti-NK1·1-FITC (RRID:AB_313392), and anti-CD3- Alexa 647 (RRID:AB_389323). Background and dead cells were excluded on the basis of size and complexity. Anti-CD45- APC-CY7 (RRID:AB_396774) was used to verify the purity of the leukocyte population. Subsequently, the cells were washed by centrifugation at 200 *g* for 10 min and resuspended in 300 μl FACS buffer. Data were analysed using a BD LSR Fortessa instrument and the FACSDiva software (BD Biosciences), with a minimum of 10,000 events acquired for each sample.

2.10. Cell culture and in vitro assays

Human primary HSC (hHCS) were isolated from fragments of normal livers obtained from optimal cadaveric liver donors, as previously described [31,32]. Human immortalized HSCs (LX2) were a kind gift from Dr. Friedman (Mount Sinai School of Medicine, New York, NY, USA). LX2 cells and hHSCs were routinely grown in DMEM culture medium (Lonza, Basel, Switzerland) supplemented with 10% foetal bovine serum (FBS) (Lonza), and 100 U/ml penicillin and streptomycin (Sigma-Aldrich). Human monocyte-derived macrophages (HMDMs) were differentiated from peripheral blood monocytes by incubation in RPMI and 10% FBS (Lonza) for 7 days, as previously described [33]. HSCs were serum-starved overnight before the following treatments were performed: 10 ng/ml TGFB1 (Preprotech), 1 μg/ml rCD5L, 25 ng/ml PDGF (Preprotech) and/or 1 μg/ml human Albumin (hSA) (Grífols, Barcelona, Spain). In these experiments, the concentration of rCD5L was chosen based on previous dose-response studies on macrophages [27]. All cells were grown at 37 °C and 5% CO_2.

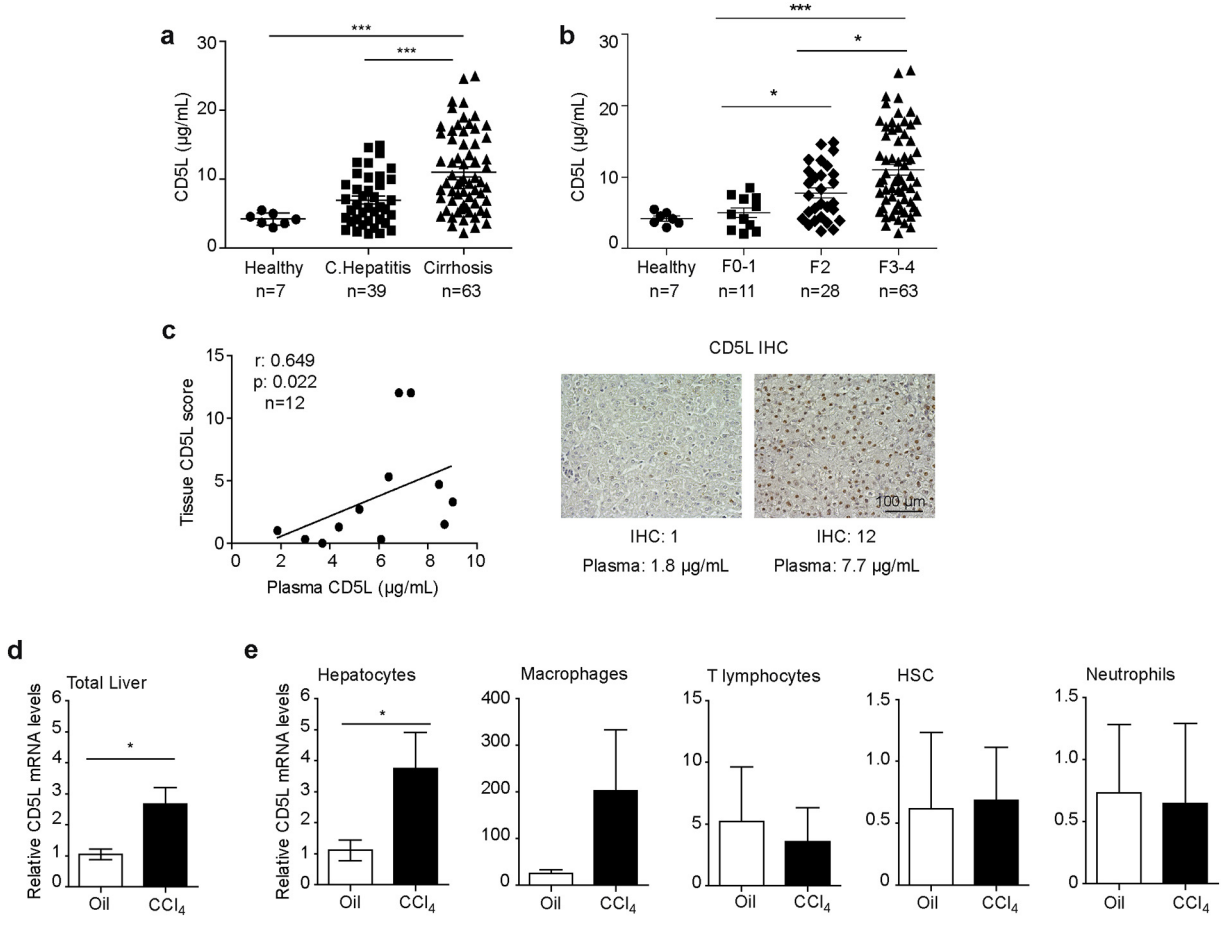

Fig. 1. Chronic liver damage induces hepatic CD5L expression. a) Plasma CD5L levels in different liver disease stages. The horizontal lines indicate the mean values ± SEM for CD5L in each group. C. hepatitis: chronic hepatitis. ***$p \leq 0{\cdot}001$ (Mann-Whitney test). b) Plasma CD5L levels according to Fibrosis-4 (FIB-4) score. F0–1: FIB-4 values <1·45; F2: FIB-4 values >1·45 and <3·25, in chronic hepatitis patients; F3–4: FIB-4 values >3.25 including all cirrhotic patients. The horizontal lines indicate the mean values ± SEM for CD5L in each group. *$p \leq 0{\cdot}05$; ***$p \leq 0{\cdot}001$ (Mann-Whitney test). c) Correlation of CD5L tissue score obtained by immunohistochemical (IHC) analysis and CD5L plasma levels from the same cirrhotic patient (left) and representative IHC images of CD5L staining in cirrhotic liver tissue and corresponding plasma levels (right). d–e) Quantitative RT-PCR determination of *Cd5l* mRNA levels. Mice were treated with carbon tetrachloride (CCl_4) or vehicle (olive oil) for two weeks. Total RNA samples were prepared from: d) whole extracts and e) isolated hepatocytes or indicated cell populations separated by flow cytometry cell sorting from one mice from each of the three independent experiments. *Cd5l* mRNA levels are displayed as relative levels (normalization to 18S and to the mean of oil group in total liver). The results are expressed as mean ± SEM of three independent experiments ($n = 4$/group). *$p \leq 0{\cdot}05$ (Mann-Whitney test). Macrophages: F4/80+; T lymphocytes: CD3+; HSC: VitA+; Neutrophils: Ly6G+.

2.11. SDS-PAGE and immunoblot analysis

Cell lysates were prepared in RIPA buffer (50 mmol/l Tris-HCl pH 8, 150 mmol/l NaCl, 1% Nonidet P-40, 0·1% SDS, 1% Triton X-100 plus proteinase inhibitors). Protein concentration was determined with a BCA protein assay reagent kit (Thermo Fisher Scientific), and sample aliquots containing 10 to 30 μg were separated by 8–10% SDS-PAGE. Western blotting procedure is described in Supplementary Methods.

2.12. RNA isolation and qPCR

For gene expression analysis by qPCR, total RNA from cells and liver tissue were extracted and reverse transcribed as detailed in the Supplementary Methods. All qPCRs were quantified using relative standard curves and normalized to the expression of GAPDH (for human genes), β-actin or 18S (for mouse genes). The primer sequences used are listed in the Supplementary Methods.

2.13. Immunofluorescence

Immunofluorescence staining was performed using MillicellEZ slides (Millipore, Billerica, MA, USA), as described in Supplementary Methods section. Confocal microscopy images were taken with a FluoView™ FV1000 Spectral Confocal microscope followed by analysis with the Zen Blue software (Carl Zeiss Microscopy GmbH).

2.14. Enzyme-linked immunosorbent assay (ELISA) for VEGF

VEGF levels in collected cell culture medium were determined with an ELISA kit (R&D Systems), following the manufacturer's protocol.

2.15. Proliferation

The effect of rCD5L on HSC proliferation was evaluated using the Cell Counting Kit 8 (CCK-8, Dojindo, Munich, Germany) and following the manufacturer's recommendations. In brief, LX2 cells and hHSCs were treated with rCD5L (1 μg/ml) in 96-well plates. Untreated cells seeded and grown in parallel were used as controls. After 96 h, proliferation was evaluated as detailed in Supplementary Methods. Viable cell number was determined using a calibration curve prepared for each cell type.

2.16. Statistical analyses

All the images show representative data from at least three independent experiments, unless otherwise indicated. Results are expressed as mean ± SEM with the number of individual experiments detailed in the Figure Legends. Statistical evaluation of multiple groups was performed using a one-way ANOVA with post-hoc Tukey test. Statistical evaluation of two groups was performed using Student's t or the Mann–Whitney test Normal distribution was assessed by d'Agostino and Pearson normality test. A p value of <0·05 was considered statistically significant.

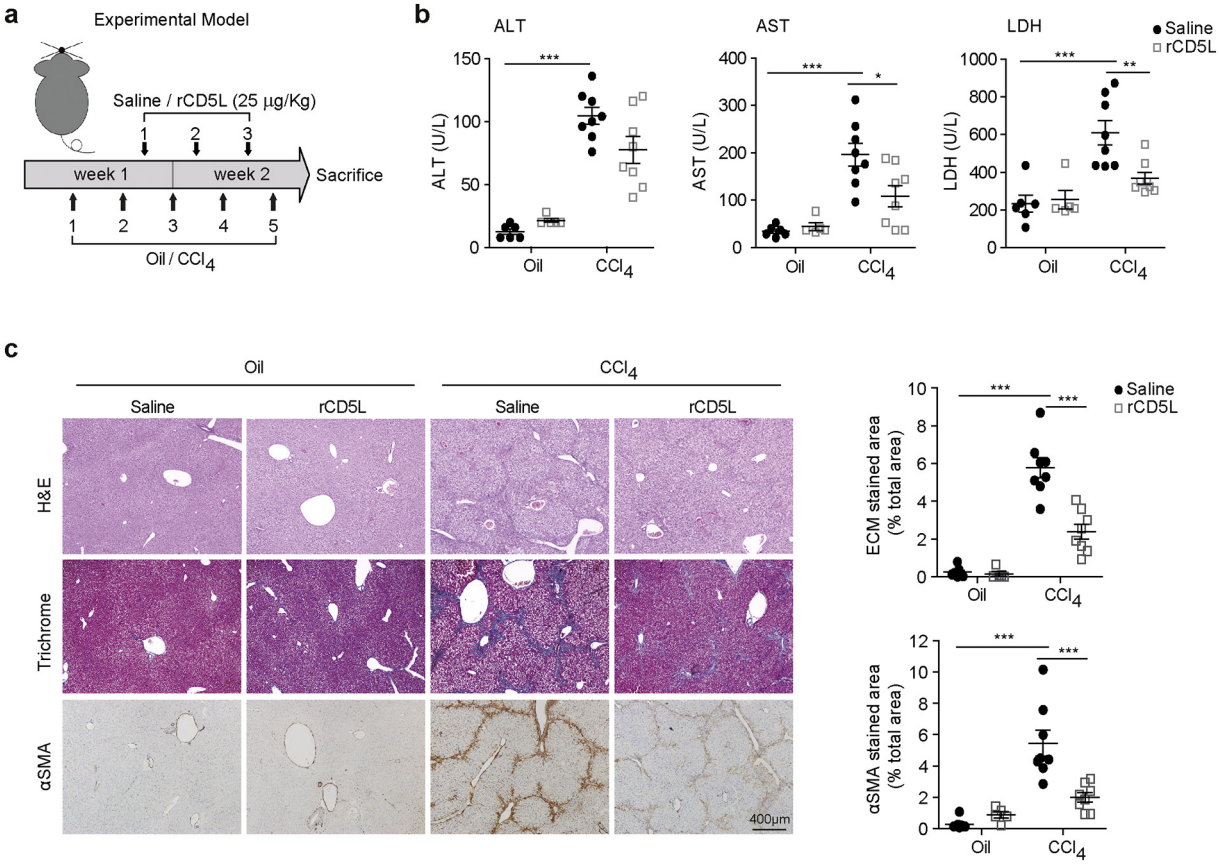

Fig. 2. rCD5L administration reduces CCl_4-induced liver damage and fibrosis in mice. a) Schematic illustration of mouse model of liver injury and rCD5L dosing. Four groups of animals were established (oil/saline $n = 8$; oil/rCD5L $n = 5$; CCl_4/saline n = 8; CCl_4/rCD5L n = 8). The animals were injected with CCl_4 or vehicle (olive oil, oil) five times over two weeks. The first treatment with rCD5L or vehicle (saline) was administered one day after the second CCl_4 injection. The mice were sacrificed 48 h after the last CCl_4 injection. After collection of blood samples, the liver was resected and preserved for further analysis. b) Levels of serum markers alanine aminotransferase (ALT), aspartate aminotransferase (AST) and lactate dehydrogenase (LDH). *$p \leq 0{\cdot}05$; **p ≤ 0·01; ***p ≤ 0·001 (Mann-Whitney test). c) Left, representative images (20×) from H&E, Masson's Trichrome and αSMA IHC staining of sections prepared from resected liver. Right, quantification of positive stained area in Trichrome and αSMA images for all cases using five random fields/ each. Results are presented as mean for each animal, in addition to overall mean ± SEM (horizontal bar). *p ≤ 0·05; **p ≤ 0·01; ***p ≤ 0·001, compared to double negative control (Mann-Whitney test).

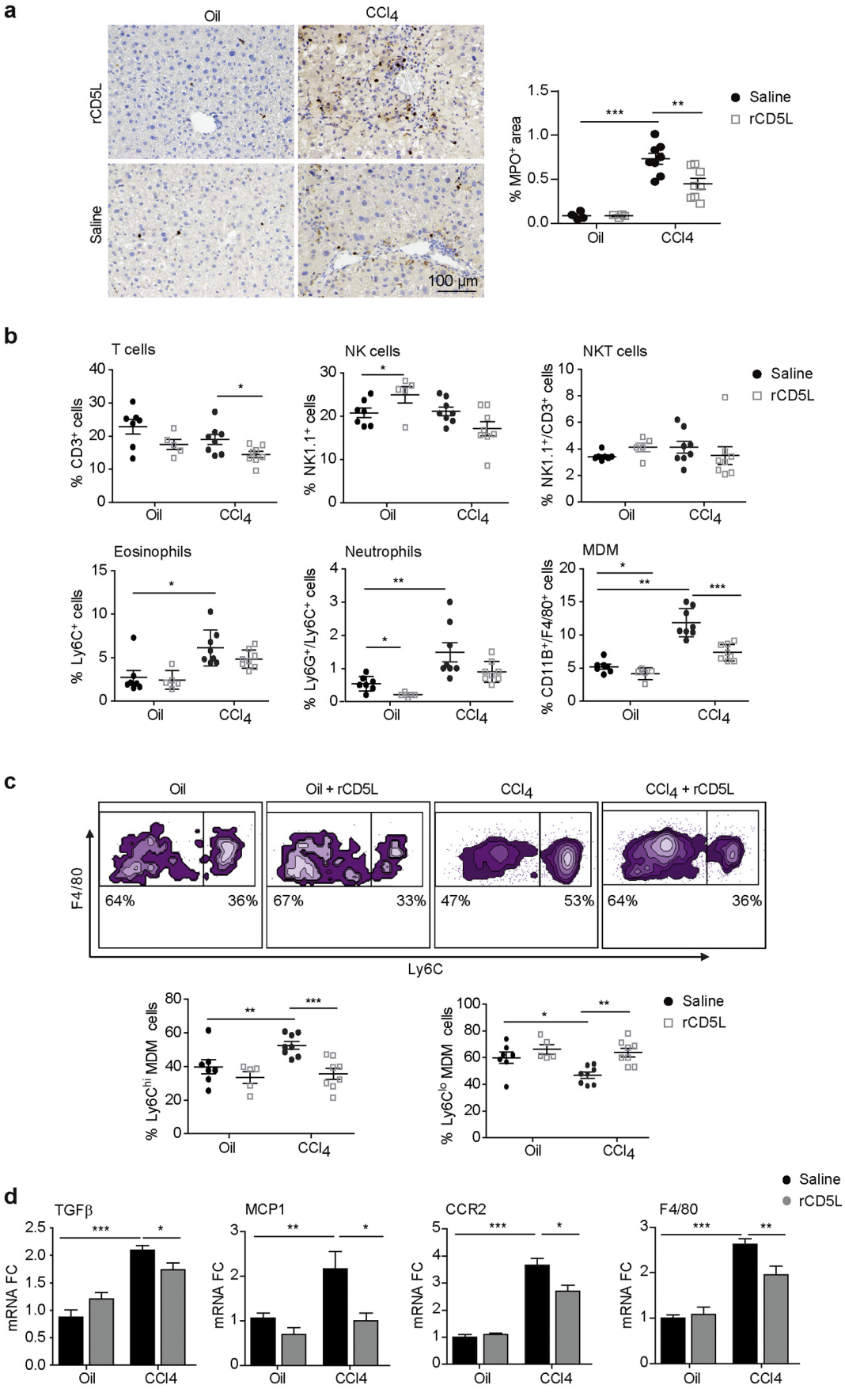
a
Oil
CCl4
rCD5L
Saline
100 μm
% MPO+ area
Saline
rCD5L
Oil
CCl4
b
T cells
% CD3+ cells
NK cells
% NK1.1+ cells
NKT cells
% NK1.1+/CD3+ cells
Eosinophils
% Ly6C+ cells
Neutrophils
% Ly6G+/Ly6C+ cells
MDM
% CD11B+/F4/80+ cells
c
Oil
Oil + rCD5L
CCl4
CCl4 + rCD5L
F4/80
Ly6C
64%
36%
67%
33%
47%
53%
64%
36%
% Ly6Chi MDM cells
% Ly6Clo MDM cells
d
TGFβ
MCP1
CCR2
F4/80
mRNA FC

All statistical analyses were performed using Graphpad Prism V.5 software.

3. Results

3.1. CD5L expression is increased in liver fibrosis

Plasma CD5L levels in patients with different stages of chronic liver disease, ranging from chronic hepatitis to cirrhosis were quantified by ELISA. The baseline clinical characteristics of these patients are shown in Table 1. Mean ± SD plasma CD5L concentration in the healthy was 4·2 ± 0·8 μg/ml, according to previous data [26] and increased with disease severity (mean μg/ml ± SD: chronic hepatitis 6·9 ± 3·6, cirrhotic, 11 ± 5·7) (Fig. 1a). Furthermore, CD5L levels in patients with advanced fibrosis (FIB-4 values >3·25, F3–4) were significantly higher than those with intermediate fibrosis (F2, FIB-4 values between 3·25 and 1·45) or non- or mild fibrosis (FIB-4 values <1·45, F0–1) patients (Fig. 1b). Similar results were obtained by using the APRI score (Supplementary Fig. 1a). CD5L plasma levels also associated with complications of cirrhosis, since they were higher in those patients with oesophagic or gastric varices and with ascites compared with those without ($p = 0·0017$ and $p = 0·0327$, respectively (Mann-Whitney test)) (Supplementary Fig. 1b). Moreover, in cirrhotic patients, we observed a negative correlation of CD5L plasma levels with albumin, prothrombin time, sodium levels, and platelet counts (Supplementary Fig. 1c). These results reveal that plasma CD5L is strongly associated with liver disease severity.

Interestingly, we observed a strong correlation between hepatic CD5L protein expression and its plasmatic levels ($p = 0·022$; $r = 0·649$ (Spearman correlation test)) in a subset of 12 patients from which both plasma and tissue samples were available (Fig. 1c), thereby suggesting a correspondence between circulating and liver tissue levels of CD5L. To further evaluate CD5L expression during hepatic fibrogenesis, we next used a well-established murine model of chronic liver injury induced by short-term carbon tetrachloride (CCl_4) [30]. Quantitative RT-PCR gene expression analysis of total liver revealed that two weeks after the initiation of liver damage, the levels of CD5L mRNA had nearly tripled (Fig. 1d). Analysis of the relative expression levels in the specific hepatic cell populations isolated by cell sorting showed that a similar increase was observed in hepatocytes and macrophages upon damage (Fig. 1e). Conversely, other cell types, such as T cells, showed no increase upon damage. Furthermore, HSCs and neutrophils showed very low, invariant levels of CD5L mRNA. In summary, these results suggest that CD5L is produced mainly by macrophages and hepatocytes and is increased upon liver damage in both mice and humans.

3.2. CD5L attenuates chronic liver injury and fibrosis by CCl_4

Next, we examined the putative role of rCD5L in preventing fibrosis *in vivo* (Fig. 2a) using an established mouse model in which hepatic damage is produced by repetitive cytotoxic CCl_4 injections. We first determined the potential effect of rCD5L administration on the liver parenchyma by measuring the plasmatic levels of hepatic enzymes ALT, AST and LDH at the end of the experiment (Fig. 2b). All three markers indicated that treatment with rCD5L significantly reduced liver damage. Moreover, H&E staining of sections prepared from resected livers showed a clear decrease in tissue damage. In this regard, trichrome staining of collagen fibers, as well as immunohistochemistry (IHC) of αSMA, revealed elevated liver fibrosis in the CCl_4-damaged group, which was significantly reduced by rCD5L treatment (Fig. 2c).

3.3. rCD5L administration reshapes the profile of recruited inflammatory cells

Fibrosis is exacerbated by the associated inflammatory response [34]. Given that CD5L acts as an anti-inflammatory mediator in macrophages [27,35], we further sought to analyse whether its hepatoprotective effect *in vivo* was mediated through additional modulation of the liver inflammatory component. In this regard, liver IHC staining of the myeloperoxidase enzyme (MPO), which is present in neutrophil granules, showed a significant decrease in neutrophil infiltration after rCD5L treatment (Fig. 3a). To further characterize the effect of rCD5L in immune cell populations, liver leukocytes were isolated and subjected to multicolour FACS analysis. Supplementary Fig. 2 shows the FACS strategy for gating and analysis. CCl_4 administration enhanced eosinophil, neutrophil and monocyte-derived macrophage (MDM) content (1·6, 2·7 and 2·2 fold, respectively), while treatment with rCD5L diminished the recruitment of T-cells and MDM cells by 60% (Fig. 3b).

Further analysis revealed a striking difference in the ratio of the two MDM subpopulations (Fig. 3c). Interestingly, the group that received rCD5L displayed an increase in the number of $Ly6C^{low}$ cells and a reduction in $Ly6C^{hi}$ cells, resulting in a similar subpopulation ratio to that found in the livers of control mice. In agreement, livers from mice treated with rCD5L showed a reduced expression of *Tgfb1*, as well as the chemokine receptor *Ccr2* and its ligand *Mcp1*, known to participate in the regulation of monocyte infiltration, and expression of *F4/80* (Fig. 3d) [36]. Taken together, our results suggest that CD5L regulates the inflammatory component in CCl_4-induced fibrosis.

3.4. CD5L inhibits HSC activation by TGFβ

Given that we observed reduced fibrosis by rCD5L administration *in vivo*, we next aimed at studying whether this protein could modulate the activity of hepatic stellate cells (HSC), the main cell type involved in fibrogenesis. We analysed CD5L mRNA and protein expression by primary human HSC (hHSCs) and an activated human hepatic stellate cell line (LX2), and compared the results with the same parameters in macrophages, used as a positive control. CD5L mRNA expression by hHSCs or LX2 cells was almost negligible and around thirty times less than that of macrophages (HMDMs) (mean relative levels ± SD 0·38 ± 0·32 hHSC, *vs.* 13·97 ± 16·62 HMDM) (Fig. 4a). In agreement, CD5L protein levels were almost undetectable in hHSCs and LX2 cells by immunofluorescence (IF) (Fig. 4b). These data are in agreement with low CD5L expression by HSCs isolated from mouse liver (Fig. 1d), and they reinforce the notion that HSCs are not an important source of CD5L. We next sought to analyse whether exogenous CD5L affects HSC activation. In this regard, although administration of rCD5L to hHSC *in vitro* induced significant changes in the expression of *Acta2, Timp1* and *IL8,* these changes were below a 1·5 fold, and were considered negligible (Fig. 4c). In addition, rCD5L did not affect hHSC

Fig. 3. rCD5L administration inhibits inflammatory infiltrate and shifts the phenotype of monocyte-derived macrophages (MDMs) in CCl_4-treated mice. a) Resected liver sections were stained with myeloperoxidase (MPO) by IHC. Left, representative images (20×) of liver sections. Right, graph depicting the mean of % stained areas in five random fields of view/animal using the Image J software. $^{**}p \le 0·01$; $^{***}p \le 0·001$ (Mann-Whitney test). b) Mononuclear cells were isolated from resected livers, and the following gating strategy and markers were used to identify cellular populations by antibody staining: CD3+ (T cells), NK1.1+ (NK cells), CD3+/NK1.1+ (NKT cells), LY6C+ (Neutrophils), LY6Cint SSChi (Eosinophils), and CD11b+/F4/80+ (MDM). The relative sizes of intrahepatic subpopulations were determined by flow cytometry. The results are presented as mean ± SEM, for each of the four treatment groups. $^{*}p \le 0·05$; $^{**}p \le 0·01$; $^{***}p \le 0·001$ (Student's *t*-test). c) Representative flow cytometry population plots of MDMs (CD11b+/F4/80+) subset analysis on the basis of Ly6C expression identified two distinct subpopulations ($Ly6C^{hi}$ and $Ly6C^{lo}$). The % of each population for each animal in the four treatment groups is indicated in the lower graphs. $^{*}p \le 0·05$; $^{**}p \le 0·01$; $^{***}p \le 0·001$ (Student's *t*-test). d) Total RNA was isolated from liver samples of each animal in the four treatment groups, and *Tgfb1*, *Mcp1*, *Ccr2*, and *F4/80* mRNA levels were determined by qRT-PCR. Graphs show mean ± SEM relative mRNA levels (normalization to β-actin and Oil). FC: fold change. $^{*}p \le 0·05$; $^{**}p \le 0·01$; $^{***}p \le 0·001$ (Mann-Whitney test).

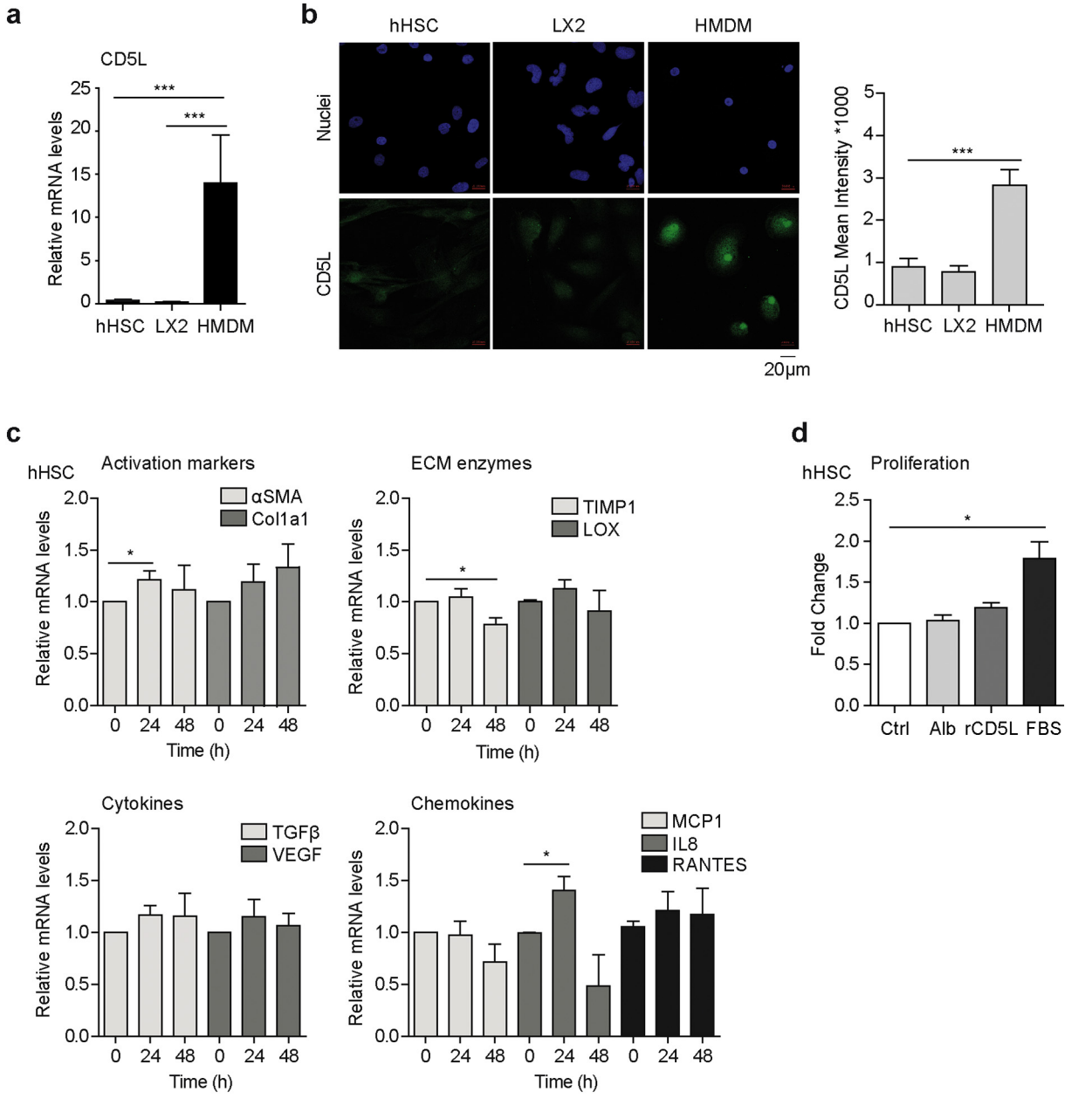

Fig. 4. CD5L does not activate hHSCs. a) Quantitative RT-PCR determination of CD5L relative mRNA levels, hHSCs and human monocyte-derived macrophage (HMDM) primary cultures from three donors, as well as LX2 cells. Mean values ± SEM from three independent experiments (normalization to GAPDH). *p ≤ 0·05; **p ≤ 0·01, compared to HMDMs (Mann-Whitney test). b) Representative immunofluorescence confocal microscopy images of the same cell cultures as in (a), with CD5L (green) and Hoechst dye staining of the nuclei (blue). Right, mean fluorescence intensity signal ± SEM of all cells in five random fields was quantified with ImageJ software. *p ≤ 0·05; **p ≤ 0·01, compared to hHSCs (Student's *t*-test). c) hHSC primary cultures from three donors were incubated with rCD5L (1 μg/ml) at the indicated time points before isolation of total RNA. The indicated mRNAs were then quantified by qRT-PCR. Data are displayed as mean relative levels ± SEM (normalization to GAPDH and to time 0). *p ≤ 0·05; **p ≤ 0·01, compared to time 0 (Student's *t*-test). d) hHSCs from three donors were seeded in individual wells containing medium (Ctrl) supplemented with Albumin (Alb) (1 μg/ml), rCD5L (1 μg/ml), or 10% FBS (FBS) as positive control for 96 h. Data show mean fold change ± SEM in cell numbers, calculated by CCK-8 staining by comparison with a standard curve of known cellular concentrations. *p ≤ 0·05, compared to Ctrl (Student's *t*-test).

proliferation (Fig. 4d). Together, our data suggest that CD5L is not significantly expressed in hHSCs nor does it induce their activation.

We next tested whether CD5L influences TGFβ-mediated HSC activation, since the latter is a potent pro-fibrogenic cytokine that targets HSCs [3]. To this end, hHSCs were pre-incubated in the presence or absence of rCD5L and then stimulated with TFGβ. The expression of a panel of genes known to be regulated by TGFβ was measured (Fig. 5a). rCD5L significantly mitigated TGFβ-induced expression of pro-fibrogenic factors, including, TGFβ and Col1a1, as well as VEGF. A similar trend was observed for the ECM regulatory glycoprotein TIMP1 mRNA and also Acta2, the gene encoding for αSMA. The inhibition of TGFβ activation was confirmed at the protein level for the Acta2 gene product αSMA (Fig. 5b) and for VEGF (Fig. 5c), by western blotting and ELISA, respectively.

3.5. CD5L inhibits the TFGβ signalling pathway by enhancing SMAD7

To explore the mechanism by which CD5L inhibits TGFβ signalling, we examined downstream mediators of this pathway. We first studied the levels of SMAD7, a key repressor of TGFβ signalling that inhibits receptor complex formation and subsequent activation of SMAD2/3 and, indirectly, ERK [1]. rCD5L treatment of hHSCs induced the expression

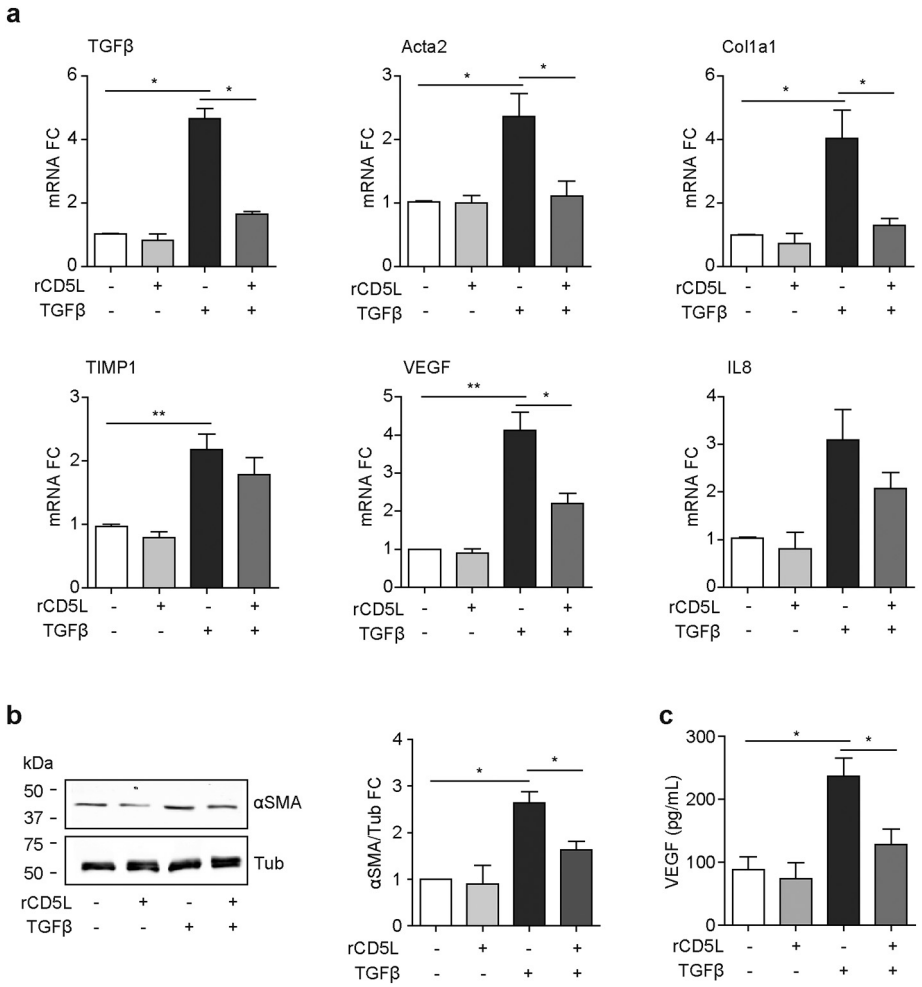

Fig. 5. rCD5L inhibits HSC responses to TGFβ. a) hHSC primary cultures were treated with rCD5L (1 μg/ml) 24 h before addition of TGFβ (10 ng/ml) or vehicle (−). Total RNA was extracted 48 h later and the levels of the indicated mRNA were assessed by qRT-PCR. The results are mean relative mRNA levels ± SEM (normalization to GAPDH and double negative control), from three donors. *p ≤ 0·05; **p ≤ 0·01 (Mann-Whitney test). FC: fold change. b) hHSCs were treated as in (A), total cell extracts were isolated and α-SMA and β-tubulin (Tub) protein levels were analysed. Left, western blot representative images from three independent determinations. Right, the intensities of the specific signals were quantified with ImageJ software, and α-SMA values were normalized to Tub. Graphs shows mean ± SEM of fold change to double negative control of three independent experiments. *p ≤ 0·05 (Student's *t*-test). FC: fold change. c) Secreted VEGF levels in media from hHSCs treated as in (a) were determined by ELISA. The results are expressed as mean ± SEM of three independent experiments of primary cultures prepared from three donors. *p ≤ 0·05 (Student's *t*-test).

of SMAD7 mRNA in a time-dependent manner (Fig. 6a). Likewise, addition of rCD5L to LX2 cells for 24 h induced a significant increase in SMAD7 protein expression (Fig. 6b). Furthermore, pre-treatment with rCD5L led to a reduction in TGFβ-mediated ERK phosphorylation (Fig. 6c). We then analysed the activation of the SMAD2/3 transcription factors, which are controlled by SMAD7 and are among the main regulators of hepatic fibrosis [9]. TGFβ induced SMAD2/3 activation (as measured by their nuclear translocation) was inhibited by rCD5L pre-treatment (Fig. 6d). This observation strongly suggests that the inhibition of the transcription of TGFβ target genes by CD5L is due to direct interference with the TGFβ pathway.

We have recently observed that CD5L induces the expression of the transcriptional regulator DNA-binding protein inhibitor ID-3 (ID3) in macrophages [35]. ID3 belongs to the inhibitor of DNA binding/differentiation (Id) family, which negatively regulates the activity of basic helix-loop-helix (bHLH) transcription factors. Interestingly, ID3, together with DNA-binding protein inhibitor ID-2 (ID2), have been shown to have opposing effects to that of TGFβ on epithelial cells [37]. Furthermore, ID2 inhibits primary rat HSC activation [38]. We confirmed the expression of ID2 and ID3 in hHSCs after treatment with TGFβ for different lengths of time. In these experiments, TGFβ produced a rapid downregulation of ID2 mRNA and upregulation of ID3 mRNA, which were maintained for up to 48 h (Fig. 6e). Interestingly, while rCD5L did not modify TGFβ-mediated enhancement of ID3 expression (Fig. 6f), it significantly inhibited ID2 downregulation at short (6 h) and long (48 h) time points (Fig. 6g). Taken together, these findings suggest that CD5L prevents the activation of the TGFβ pathway in HSCs by promoting an increase in the expression of SMAD7 and preventing SMAD2/3 nuclear translocation, as well as ID2 loss.

4. Discussion

This study demonstrates, for the first time, the functional involvement of CD5L in liver fibrosis. Elevated levels of circulating CD5L and its association with poor liver functions have been reported in liver cirrhosis [22–26]. Our data reinforce these results and confirm that circulating levels of CD5L are an indicator of liver damage, specifically fibrosis. Moreover, we provide a cut-off for the potential usefulness of measuring CD5L levels in clinical practice as a biomarker for fibrosis. In addition, the positive correlation between CD5L cirrhotic liver expression and the plasma levels of this protein suggest that the liver is the main source of CD5L in these settings and that CD5L is expressed as a local response to injury. In agreement, CCl_4-induced mouse liver damage caused a significant increase in hepatic *Cd5l* expression. One could hypothesize that the rise in CD5L during liver disease is an

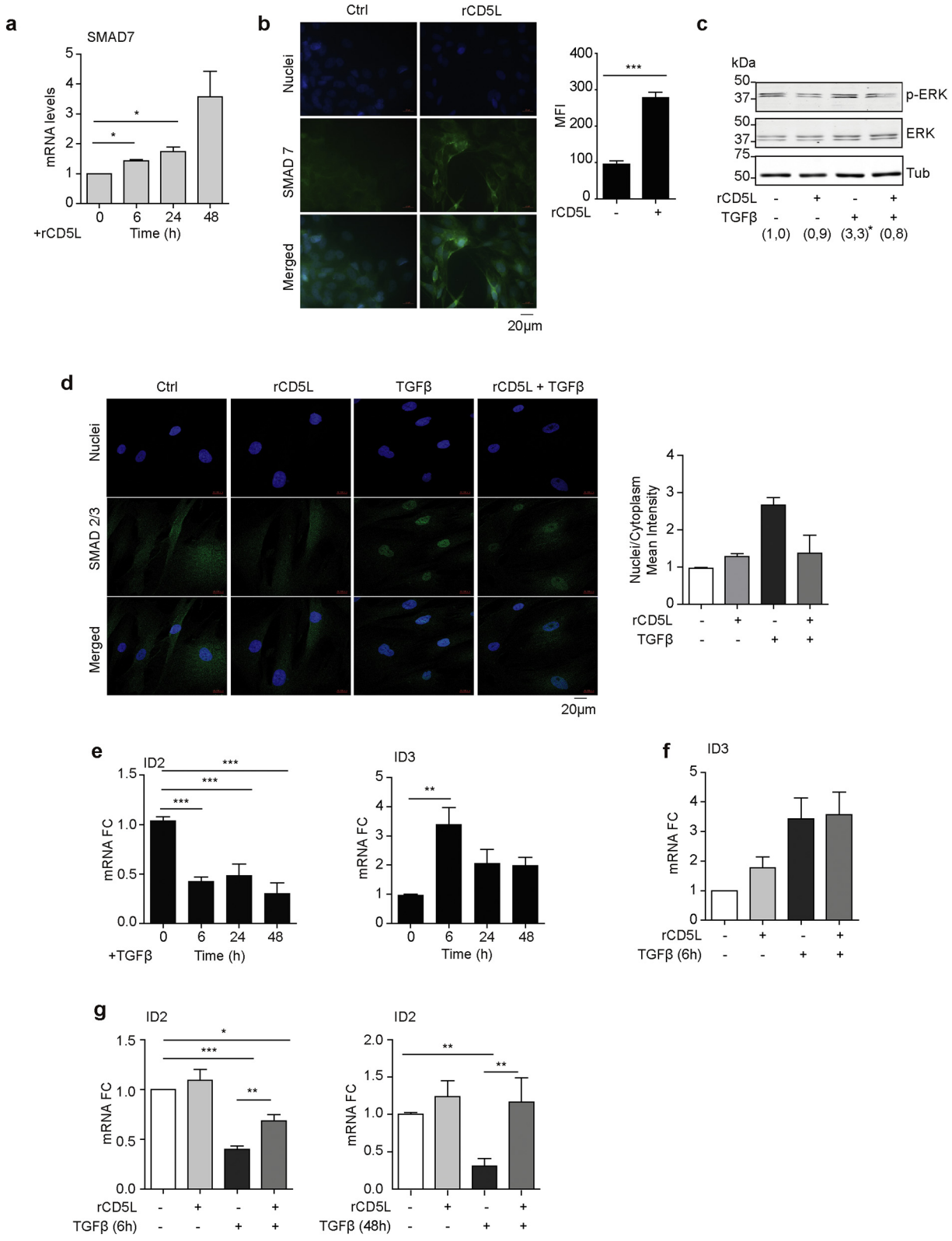

Fig. 6. CD5L regulates individual components of the TGFβ pathway. a) rCD5L (1 μg/ml) was added to hHSC primary cultures at the indicated time points before isolation of total RNA. Then, SMAD7 mRNA levels were quantified by qRT-PCR. Data are mean of three independent experiments and are shown as relative levels (normalization to GAPDH and to time 0). *p ≤ 0·05 (Student's *t*-test). b) LX2 cultures were incubated with rCD5L (1 μg/ml) for 24 h. Representative immunofluorescence confocal images of SMAD7 (green), and Hoechst nuclei staining (blue). Right, the mean ± SEM Mean Fluorescence Intensity of all cells in five random fields was quantified with Image J software. ***p ≤ 0·0001 (Student's *t*-test). c) Representative images from three independent Western blot determinations of P-ERK1/2, ERK1/2 and β-tubulin (β-tub) levels in total protein extracts from hHSCs. Where marked, rCD5L (1 μg/ml) was added 24 h before initiation of treatment for 1 h with TGFβ (10 ng/ml). The intensities of the specific signals were quantified with ImageJ software and the averages of P-Erk1/2, normalized to Erk1/2 and double negative control are shown below the image. d) hHSC cultures were incubated with rCD5L (1 μg/ml) for 24 h before treatment with TGFβ (10 ng/ml) for 15 min. Representative immunofluorescence confocal microscopy images of SMAD2/3 staining (green), with Hoechst dye staining of the nuclei (blue). Right, the mean ± SEM nuclear/cytoplasm signal ratios of all cells in five random fields were quantified for SMAD2/3 with ImageJ software. e–g) Quantitative RT-PCR determination of DNA-binding protein inhibitors ID2 and ID3 mRNA levels. Data are the mean ± SEM of three independent experiments of hHSC primary cultures from three donors, displayed as relative levels (normalization to GAPDH and time 0). e) Effect of TGFβ (10 ng/ml) over time. f-g rCD5L (1 μg/ml) was added 24 h before initiation of 6- or 48-h treatment with TGFβ (10 ng/ml) or vehicle (−). *p ≤ 0·05; **p ≤ 0·01; ***p ≤ 0·001 (Student's *t*-test). FC: fold change.

adaptive response to liver damage and fibrosis that seeks to counteract inflammatory signalling and the profibrotic effect of TGFβ.

To answer these questions, we used an established *in vivo* model of moderate fibrosis. Under these settings, administration of rCD5L had a clear protective effect on liver injury, as well as on the inflammatory response. Our results are in line with a key role of several immune mediators, such as Pentraxin-3 [32], Gas6 [39] and the NOD-like receptor protein 3 (NLRP3) [40], among others, as regulators of liver fibrosis. Our results further suggest that hepatic CD5L protein exerts its protective effect on fibrosis by a combination of mechanisms, including protecting from damage, and preventing fibrosis as well as immune cell infiltration. To the best of our knowledge, this is the first study to report a role for CD5L in preventing neutrophil and MDM infiltration in the inflamed liver. Remarkably, in the present study, we also found that CD5L shifted the phenotype of recruited macrophages from Ly6C^{hi} to Ly6C^{low}. This is in agreement with a role for this protein in modulating macrophage behaviour in multiple settings [10]. Recent studies have shown that MDM infiltration of the liver and its phenotype after chronic injury is related to the progression of inflammation and fibrosis [41–43]. In particular, the balance between two subsets of MDMs, defined by abundance of the Ly6C surface marker in CD11b+, F4/80+ cells, correlated with the amount of murine liver fibrosis regression. While Ly6C^{hi} MDMs promoted fibrogenesis, Ly6C^{low} cells were important for the resolution of liver fibrosis [44]. It is interesting that a previous study identified *Cd5l* as one of the genes overexpressed in regenerative Ly6C^{low} macrophages [44]. In this regard, our results may be of critical relevance in the context of macrophage activity in chronic liver disease.

Our results further reveal that HSCs are a novel cellular target of CD5L. Early studies proposed that CD5L exerted distinct functions depending on the target cell types and/or its combined effects with other cytokines [45]. In this regard, besides acting on macrophages [10,35], CD5L plays diverse autocrine functions in hepatocytes [21], Th17 cells [17], and the retinal pigment epithelium [19], among other cell types. Additionally, it acts in a paracrine fashion on other cell types, namely adipocytes, where it is internalized and modifies metabolic activity [46]. Therefore, our data reinforce the notion that CD5L may be a pleiotropic protein that controls the activity of numerous cell types.

The novel finding that CD5L inhibits TGFβ action on HSCs and signalling is of great relevance in the context of liver disease, given the important role of TGFβ in fibrogenesis. It also provides a new mechanism by which CD5L slows down activation, through a combined action of enhancing SMAD7 activity and ID2 transcription factor levels. The role of SMAD7 as a negative feedback regulator of TGFβ in HSCs is well established. On the other hand, ID2 is a downstream target of BMP7 signalling, which has been proposed as a pivotal factor inhibiting TGFβ signalling and regulating hepatic fibrogenesis [9]. Therefore, it is possible that CD5L-mediated inhibition of TGFβ in HSCs occurs partially *via* the enhancement of the BMP7 signalling pathway. Our results shed light on the cross-talk between BMP and TFGβ signalling, a current focus of intense research efforts [9].

In summary, the results of the present study show, for the first time, the involvement of CD5L in reducing HSC activation, liver injury and inflammation during CCl_4 damage. On the basis of our results, CD5L emerges as a key player in fibrosis in the setting of chronic liver disease.

Funding sources

This work was supported by grants from the *Fundació la Marató de TV3* (MTV3 2013-3610), AGAUR (2016 PROD 00094, 2017-SGR-490) to MRS, CSIC (PIE-201720E092) and also from the *Instituto de Salud Carlos III* (ISCIII), and ERDFs from the EU, 'Una manera de hacer Europa', (PI10/01565, PI13/1906, PI16/0974, PI13/02340, PI09/00751 and PI17/00673 to MRS, CA, and PS-B, respectively and PI14/00703 to LK). MRS, PS-B, CA, and CB were supported by the Miguel Servet (CPII14/00021; CPII15/00041), Ramón y Cajal (RYC-2010-07249), and Juan de la Cierva (FJCI-2014-20,505) programs, respectively. The IGTP is member of the CERCA network of institutes. The funders had no role in study design, data collection, data analysis, interpretation, or writing of the report.

Conflicts of interest

A patent protecting monoclonal antibodies used herein for ELISA studies has been submitted to the European Patent Office.

Author contributions

CB, GA: designed and performed research, analysed data and wrote the paper; LP, LS, MGG, LK, ET, AO: designed and performed research and analysed data; HM, MS, CA, PS, designed research, contributed patient samples and clinical databases, and analysed data. IS: contributed patient samples and clinical databases. MRS: designed research, analysed data, and wrote the paper.

Acknowledgements

We thank Marco Fernández, Gerard Requena, and Pilar Armengol from the Flow Cytometry and Microscopy Units at the IGTP.

Appendix A. Supplementary data

Supplementary data to this article can be found online at https://doi.org/10.1016/j.ebiom.2019.04.052.

References

[1] Tsuchida T, Friedman SL. Mechanisms of hepatic stellate cell activation. Nat Rev Gastroenterol Hepatol 2017;14:397–411. https://doi.org/10.1038/nrgastro.2017.38.
[2] Bataller R, Brenner DA. Liver fibrosis. J Clin Invest 2005;115:209–18. https://doi.org/10.1172/JCI24282.
[3] Hellerbrand C, Stefanovic B, Giordano F, Burchardt ER, Brenner DA. The role of TGFβ1 in initiating hepatic stellate cell activation in vivo. J Hepatol 1999;30:77–87. https://doi.org/10.1016/S0168-8278(99)80010-5.
[4] Friedman SL. Mechanisms of disease: mechanisms of hepatic fibrosis and therapeutic implications. Nat Rev Gastroenterol Hepatol 2004;1:98–105. https://doi.org/10.1038/ncpgasthep0055.
[5] Gauldie J, Bonniaud P, Sime P, Ask K, Kolb M. TGF-β, Smad3 and the process of progressive fibrosis. Biochem Soc Trans 2007;35:661–4. https://doi.org/10.1042/BST0350661.
[6] Nakagawa T, Li JH, Garcia G, Mu W, Piek E, Böttinger EP, et al. TGF-beta induces proangiogenic and antiangiogenic factors via parallel but distinct Smad pathways. Kidney Int 2004;66:605–13. https://doi.org/10.1111/j.1523-1755.2004.00780.x.
[7] Reimann T, Hempel U, Krautwald S, Axmann A, Scheibe R, Seidel D, et al. Transforming growth factor-β1 induces activation of Ras, Raf-1, MEK and MAPK in rat hepatic stellate cells. FEBS Lett 1997;403:57–60. https://doi.org/10.1016/S0014-5793(97)00024-0.
[8] Derynck R, Zhang YE. Smad-dependent and Smad-independent pathways in TGF-beta family signalling. Nature 2003;425:577–84. https://doi.org/10.1038/nature02006.
[9] Herrera B, Addante A, Sánchez A. BMP signalling at the crossroad of liver fibrosis and regeneration. Int J Mol Sci 2018;19. https://doi.org/10.3390/ijms19010039.
[10] Sanjurjo L, Aran G, Roher N, Valledor A, Sarrias M-R. AIM/CD5L: a key protein in the control of immune homeostasis and inflammatory disease. J Leukoc Biol 2015;98:173–84. https://doi.org/10.1189/jlb.3RU0215-074R.
[11] Armengol C, Bartolí R, Sanjurjo L, Serra I, Amézaga N, Sala M, et al. Role of scavenger receptors in the pathophysiology of chronic liver diseases. Crit Rev Immunol 2013;33:57–96.
[12] Zou T, Garifulin O, Berland R, Boyartchuk VL. Listeria monocytogenes infection induces prosurvival metabolic signaling in macrophages. Infect Immun 2011;79:1526–35. https://doi.org/10.1128/IAI.01195-10.
[13] Valledor AF, Hsu L, Ogawa S, Sawka-Verhelle D, Karin M, Glass CK. Activation of liver X receptors and retinoid X receptors prevents bacterial-induced macrophage apoptosis. Proc Natl Acad Sci U S A 2004;101:17813–8. https://doi.org/10.1073/pnas.0407749101.
[14] Sanjurjo L, Amézaga N, Vilaplana C, Cáceres N, Marzo E, Valeri M, et al. The scavenger protein apoptosis inhibitor of macrophages (AIM) potentiates the antimicrobial response against Mycobacterium tuberculosis by enhancing autophagy. PLoS One 2013;8:e79670.
[15] Kroesen VM, Rodríguez-Martínez P, García E, Rosales Y, Díaz J, Martín-Céspedes M, et al. A beneficial effect of low-dose aspirin in a murine model of active tuberculosis. Front Immunol 2018;9. https://doi.org/10.3389/fimmu.2018.00798.
[16] Arai S, Shelton JM, Chen M, Bradley MN, Castrillo A, Bookout AL, et al. A role for the apoptosis inhibitory factor AIM/Spalpha/Api6 in atherosclerosis development. Cell Metab 2005;1:201–13 [doi:S1550-4131(05)00055-0 [pii]\r10.1016/j.cmet.2005.02.002].

[17] Wang C, Yosef N, Gaublomme J, Wu C, Lee Y, Clish CB, et al. CD5L/AIM regulates lipid biosynthesis and restrains Th17 cell pathogenicity. Cell 2015;163:1413–27.
[18] Li Y, Qu P, Wu L, Li B, Du H, Yan C. Api6/AIM/Sp{alpha}/CD5L overexpression in alveolar type II epithelial cells induces spontaneous lung adenocarcinoma. Cancer Res 2011;71:5488–99. https://doi.org/10.1158/0008-5472.CAN-10-4225.
[19] Iannaccone A, Hollingsworth TJ, Koirala D, New DD, Lenchik NI, Beranova-Giorgianni S, et al. Retinal pigment epithelium and microglia express the CD5 antigen-like protein, a novel autoantigen in age-related macular degeneration. Exp Eye Res 2017;155:64–74. https://doi.org/10.1016/j.exer.2016.12.006.
[20] Haruta I, Kato Y, Hashimoto E, Minjares C, Kennedy S, Uto H, et al. Association of AIM, a novel apoptosis inhibitory factor, with hepatitis via supporting macrophage survival and enhancing phagocytotic function of macrophages. J Biol Chem 2001;276:22910–4.
[21] Aran G, Sanjurjo L, Bárcena C, Simon-Coma M, Téllez É, Vázquez-Vitali M, et al. CD5L is upregulated in hepatocellular carcinoma and promotes liver cancer cell proliferation and antiapoptotic responses by binding to HSPA5 (GRP78). FASEB J 2018;32:3878–91. https://doi.org/10.1096/fj.201700941RR.
[22] Gangadharan B, Antrobus R, Dwek RA, Zitzmann N. Novel serum biomarker candidates for liver fibrosis in hepatitis C patients. Clin Chem 2007;53:1792–9. https://doi.org/10.1373/clinchem.2007.089144.
[23] Sarvari J, Mojtahedi Z, Taghavi SAR, Kuramitsu Y, Shamsi Shahrabadi M, Ghaderi A, et al. Differentially expressed proteins in chronic active hepatitis, cirrhosis, and HCC related to HCV infection in comparison with HBV infection: a proteomics study. Hepat Mon 2013;13:e8351.
[24] Mera K, Hirofumi U, Seiichi M, Akio I, Yozo Y, Tsuyoshi N, et al. Serum levels of apoptosis inhibitor of macrophage are associated with hepatic fibrosis in patients with chronic hepatitis C. BMC Gastroenterol 2014;14:1–10. https://doi.org/10.1186/1471-230X-14-27.
[25] Gray J, Chattopadhyay D, Beale GS, Patman GL, Miele L, King BP, et al. A proteomic strategy to identify novel serum biomarkers for liver cirrhosis and hepatocellular cancer in individuals with fatty liver disease. BMC Cancer 2009;9:271. https://doi.org/10.1186/1471-2407-9-271.
[26] Yamazaki T, Mori M, Arai S, Tateishi R, Abe M, Ban M, et al. Circulating AIM as an indicator of liver damage and hepatocellular carcinoma in humans. PLoS One 2014;9:e109123.
[27] Sanjurjo L, Amézaga N, Aran G, Naranjo-Gómez M, Arias L, Armengol C, et al. The human CD5L/AIM-CD36 axis: a novel autophagy inducer in macrophages that modulates inflammatory responses. Autophagy 2015;11:487–502. https://doi.org/10.1080/15548627.2015.1017183.
[28] Galfre G, Howe SC, Milstein C, Butcher GW, Howard JC. Antibodies to major histocompatibility antigens produced by hybrid cell lines. Nature 1977;266:550–2.
[29] Harlow E, Lane D. Antibodies: a laboratory manual. Cold Spring Harbor, New York: Cold Spring Harbor Laboratory Press; 1988.
[30] Affo S, Morales-Ibanez O, Rodrigo-Torres D, Altamirano J, Blaya D, Dapito DH, et al. CCL20 mediates lipopolysaccharide induced liver injury and is a potential driver of inflammation and fibrosis in alcoholic hepatitis. Gut 2014;63:1782–92. https://doi.org/10.1136/gutjnl-2013-306098.
[31] Affò S, Dominguez M, Lozano JJ, Sancho-Bru P, Rodrigo-Torres D, Morales-Ibanez O, et al. Transcriptome analysis identifies TNF superfamily receptors as potential therapeutic targets in alcoholic hepatitis. Gut 2013;62:452–60. https://doi.org/10.1136/gutjnl-2011-301146.
[32] Perea L, Coll M, Sanjurjo L, Blaya D, Taghdouini AE, Rodrigo-Torres D, et al. Pentraxin-3 modulates lipopolysaccharide-induced inflammatory response and attenuates liver injury. Hepatology 2017;66:953–68. https://doi.org/10.1002/hep.29215.
[33] Amézaga N, Sanjurjo L, Julve J, Aran G, Pérez-Cabezas B, Bastos-Amador P, et al. Human scavenger protein AIM increases foam cell formation and CD36-mediated oxLDL uptake. J Leukoc Biol 2014;95:509–20. https://doi.org/10.1189/jlb.1212660.
[34] Koyama Y, Brenner DA. Liver inflammation and fibrosis. J Clin Invest 2017;127:55–64. https://doi.org/10.1172/JCI88881.
[35] Sanjurjo L, Aran G, Téllez É, Amézaga N, Armengol C, López D, et al. CD5L promotes M2 macrophage polarization through autophagy-mediated upregulation of ID3. Front Immunol 2018;9. https://doi.org/10.3389/fimmu.2018.00480.
[36] Baeck C, Wei X, Bartneck M, Fech V, Heymann F, Gassler N, et al. Pharmacological inhibition of the chemokine C-C motif chemokine ligand 2 (monocyte chemoattractant protein 1) accelerates liver fibrosis regression by suppressing Ly-6C $^{+}$ macrophage infiltration in mice: BAECK ET AL. Hepatology 2014;59:1060–72. https://doi.org/10.1002/hep.26783.
[37] Kowanetz M, Valcourt U, Bergstro R, Heldin C, Moustakas A. Id2 and Id3 define the potency of cell proliferation and differentiation responses to transforming growth factor [illegible] and bone morphogenetic protein. Society 2004;24:4241–54. https://doi.org/10.1128/MCB.24.10.4241.
[38] Tajima K, Terai S, Takami T, Kawaguchi K, Okita K, Sakaida I. Importance of inhibitor of DNA binding/differentiation 2 in hepatic stellate cell differentiation and proliferation. Hepatol Res 2007;37:647–55. https://doi.org/10.1111/j.1872-034X.2007.00089.x.
[39] Bárcena C, Stefanovic M, Tutusaus A, Joannas L, Menéndez A, García-Ruiz C, et al. Gas6/Axl pathway is activated in chronic liver disease and its targeting reduces fibrosis via hepatic stellate cell inactivation. J Hepatol 2015;63:670–8. https://doi.org/10.1016/j.jhep.2015.04.013.
[40] Mridha AR, Wree A, Robertson AAB, Yeh MM, Johnson CD, Van Rooyen DM, et al. NLRP3 inflammasome blockade reduces liver inflammation and fibrosis in experimental NASH in mice. J Hepatol 2017;66:1037–46. https://doi.org/10.1016/j.jhep.2017.01.022.
[41] Karlmark KR, Weiskirchen R, Zimmermann HW, Gassler N, Ginhoux F, Weber C, et al. Hepatic recruitment of the inflammatory Gr1+ monocyte subset upon liver injury promotes hepatic fibrosis. Hepatology 2009;50:261–74. https://doi.org/10.1002/hep.22950.
[42] Zimmermann HW, Seidler S, Nattermann J, Gassler N, Hellerbrand C, Zernecke A, et al. Functional contribution of elevated circulating and hepatic non-classical CD14+CD16+ monocytes to inflammation and human liver fibrosis. PLoS One 2010;5:e11049. https://doi.org/10.1371/journal.pone.0011049.
[43] Duffield JS, Forbes SJ, Constandinou CM, Clay S, Partolina M, Vuthoori S, et al. Selective depletion of macrophages reveals distinct, opposing roles during liver injury and repair. J Clin Invest 2005;115:56–65. https://doi.org/10.1172/JCI22675.
[44] Ramachandran P, Pellicoro A, Vernon MA, Boulter L, Aucott RL, Ali A, et al. Differential Ly-6C expression identifies the recruited macrophage phenotype, which orchestrates the regression of murine liver fibrosis. Proc Natl Acad Sci U S A 2012;109:E3186–95. https://doi.org/10.1073/pnas.1119964109.
[45] Yusa S, Ohnishi S, Onodera T, Miyazaki T. AIM, a murine apoptosis inhibitory factor, induces strong and sustained growth inhibition of B lymphocytes in combination with TGF-beta1. Eur J Immunol 1999;29:1086–93 [doi:10.1002].
[46] Kurokawa J, Arai S, Nakashima K, Nagano H, Nishijima A, Miyata K, et al. Macrophage-derived AIM is endocytosed into adipocytes and decreases lipid droplets via inhibition of fatty acid synthase activity. Cell Metab 2010;11:479–92. https://doi.org/10.1016/j.cmet.2010.04.013.